Heliyon 10 (2024) e25246

Contents lists available at ScienceDirect

Heliyon

journal homepage: www.cell.com/heliyon

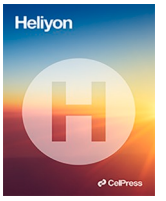

Research article

"Synthesis and characterization of a novel pyridinium iodide-tagged Schiff base and its metal complexes as potential ACHN inhibitors"

Pranesh Rai [a], Ankita Dutta [b], Anoop Kumar [b], Biswajit Sinha [a,*]

[a] Department of Chemistry, University of North Bengal, Darjeeling, 734013, India
[b] Department of Biotechnology, University of North Bengal, Darjeeling, 734013, India

ARTICLE INFO

Keywords:
Pyridinium iodide-tagged Schiff base
Distorted square planar Cu (II)-complex
Tetrahedral Zn (II) and Cd (II)-complexes
Cytotoxicity
IC_{50}
ROS assay

ABSTRACT

In quest of developing an efficient and effective drug against the ACHN human renal adenocarcinoma cell line herein, we report the synthesis and characterization of a novel Pyridinium iodide-tagged Schiff base (5) and its Cu (II)/Zn (II)/Cd (II)-complexes (6). The synthesized compounds are well characterized by Elemental analysis, UV–Visible, FTIR, Magnetic Susceptibility, NMR, HRMS, MALDI, and PXRD techniques. They were then subsequently tested on the ACHN cell lines using MTT assays and their IC_{50} values were determined, followed by their ROS production capacity. Among the tested compounds Zn (II)-complex 6(b) was found to be the most potent one with a minimum IC_{50} value while the ligand (5) was the least.

1. Introduction

Even though Paul Walden reported the first Ionic Liquid (IL) "Ethyl ammonium nitrate" in 1914 [1], Ionic liquids (ILs) however, have received wide attention only during the past two decades. The number of research papers published on ILs has drastically increased from a few numbers in the year 1996 to more than 5000 in the year 2016, surpassing the overall annual growth rates of some popular research areas. This firmly indicates that more and more researchers are involved in studying ILs with plentiful outcomes. Multidisciplinary research on ILs is emerging such as in the field of material science, chemical engineering, chemical synthesis, environmental science, and medicinal chemistry. They can show numerous useful properties such as low vapor pressure, thermal stability, potential to dissolve different substrates, high electrical conductivity, etc. An important feature of ILs is the tenability of their physical and chemical properties by varying the combination of cations and anions. Usually, large organic cations and smaller anions are designed to prepare useful ILs. Although, most of the works on ILs highlight their use as a reaction media in organic synthesis, these liquids are gradually drawing attention in the field of inorganic medicinal and material chemistry a lot. The concept of functionalized ionic liquid (FILs), by introducing additional functional group as a part of cation or anion, has presently become a subject of interest. There is a huge possibility of chemical structure modifications through the incorporation of specific functionality. Such FILs can interact with a metal center and contribute to enhanced stability of metal salts. Such metal-containing ILs are considered as promising new materials that combine the feature of ILs with additional intrinsic magnetic, catalytic, biological and spectroscopic properties depending on the incorporated metal ion [2–7].

Although these ILs are used successfully as solvents and catalysts in many reactions [4,8], there are good number of research

* Corresponding author.
E-mail address: biswachem@gmail.com (B. Sinha).

https://doi.org/10.1016/j.heliyon.2024.e25246
Received 5 November 2023; Received in revised form 23 January 2024; Accepted 23 January 2024
Available online 28 January 2024

articles which describes their biological activities such as antibacterial, antifungal, cytotoxicity, antioxidant properties [9–18]. Some common ILs contains imidazolium, pyridinium, pyrrolidinium moieties as their cationic part [19]. After a rigorous literature studies, it is found that pyridinium moiety containing ILs can be explored more, although several pyridinium containing ILs are reported in literature. Some of them are 1-(10-aminodecyl) pyridinium salt [20], polymeric 3-alkylpyridinium salts [21], 12-methacryleyloxy-dodecylpyridinium bromide [21], L-threoC6-pyridinium-ceramide-bromide [22] which shows cytotoxicity activity against different cell lines.

On the other hand, Schiff's bases are versatile pharmacophore having an azomethine linkage (C═N) generally formed by condensation of the primary amines with a carbonyl compound. The common structural property of Schiff's Bases is the presence of azomethine group (C═N) in their structure, with the general formula RHC═NR' (Where R and R′ are alkyl, aryl, cycloalkyl or heterocyclic groups). Schiff bases, usually formed by the condensation of a primary amine with an aldehyde are one of the most prevalent ligands in coordination chemistry. Schiff bases containing hetero-atoms such as nitrogen, oxygen and Sulphur are of special interest due to their different ways of bonding with transition metal ions. They have been reported to exhibit a variety of biological activities due to the presence of azomethine linkage (C═N) [23–31,38–41]. Transition metal complexes of Schiff bases carrying nitrogen and other donor sites have a variety of applications including biological, medicinal and analytical in addition to their vital role in organic synthesis and catalysis [23–32].

On combining IL with Schiff base, we get IL-tagged Schiff Base ligand system which represents a class of modified Schiff base ligand system formed by the condensation between the ionic liquid molecule containing amine or carbonyl group and the carbonyl or the amine molecule by suitably choosing, with a huge role to play in inorganic chemistry, organic chemistry, environmental chemistry, material chemistry, and medicinal chemistry as imply by the literature studies [7–12]. We use this modified Schiff base ligand system to synthesize metal complexes as several such metal complexes are reported in literature [8–10,32–37]. Herein, we thus report the synthesis and characterization of novel 3-((2-(2, 4-dinitrophenyl) hydrazinylidene) methyl)-1-methylpyridin-1-ium iodide as such ligand (5) system and its Cu (II)/Zn (II)/Cd (II)-complexes (6a, 6b, 6c).

Taking notes, the presence of biologically active azomethine linkage (C═N), pyridinium moiety, and metal ions the biological activities of the four synthesized compounds were evaluated [38–43]. However, we kept ourself confined within the cytotoxicity and reactive oxygen species (ROS) production activities of the synthesized compounds. Among the several types of cancer, we opted for kidney cancer thus its ACHN cell line for our studies. This kidney cancer is the 13th most prevalent disease globally, taking responsibility for 2–4 % of all malignancies [37]. The cytotoxicity activities of the synthesized compounds were in accordance with their ROS production ability.

2. Experimental

All the required reagents (reagent grade) and solvents (analytical grade) were purchased from Spectro chem, Hi media, Sigma-Aldrich, TCI Chemicals (India) and Merck India. All the reagents were used without further purification however, the solvents were distilled and dried before their use.

a. General methods and materials

3-carboxaldehyde pyridine (Sigma-Aldrich), methyl iodide (Sigma-Aldrich), 2,4-DNP (SRL), hydrated $Cu(OAc)_2$ (SRL), hydrated $Zn(OAc)_2$ (SRL), hydrated $Cd(OAc)_2$ (SRL), acetone, methanol, and dilute hydrochloric acid were used. The pyridinium salt (3) was synthesized as reported in the literature [48]. The ligand (5) and its Cu (II)/Zn (II)/Cd (II)-complexes [6(a)/6(b)/6(c)] were prepared by following conventional methods. The ACHN human renal adenocarcinoma cells were purchased from National Center for Cell Science, Pune, India. Media components and MTT used for the studies were purchased from Hi-Media Laboratory Pvt. Ltd.

Elemental analysis was done using PerkinElmer (Model 240C) analyzer. UV–Visible spectra were recorded in the Agilent 8453 spectrophotometer, with an uncertainty of wavelength resolution of ± 0.5 nm. Automated thermostat kept the temperature of the cell fixed. FTIR spectra were recorded on a PerkinElmer Spectrum FTIR Spectrometer using the KBr pellets at room temperature. Magnetic susceptibility balance was used to measure magnetic susceptibilities at room temperature (Magway MSB MK1, Sherwood Scientific Ltd.). NMR-spectra were recorded on Bruker 400 spectrometer operating at 400 MHz in DMSO-d_6. HRMS were obtained on Bruker microTOF-Q II spectrometer. MALDI were recorded in Bruker Daltonics auto flex TOF/TOF instrument while PXRD in PANalytical X-ray Diffractometer using Cu-κα radiation (1.54 A^0).

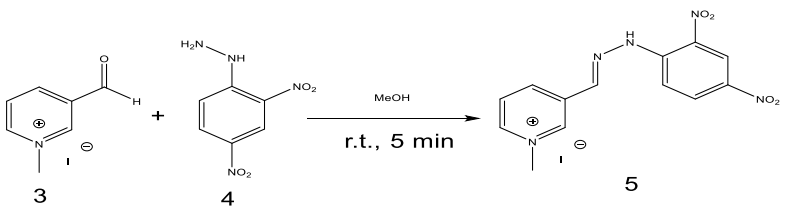

Scheme 2. Synthesis of IL-tagged Schiff base (5).

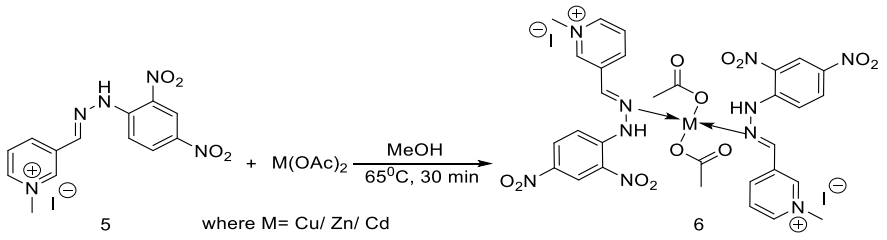

Scheme 3. Synthesis of IL-tagged Schiff base metal complex (6).

b. Synthesis

i. Pyridinium IL (3)

The compound (3) was prepared following the procedure given in the literature [44]. A mixture of 3-pyridine carboxaldehyde (1) (1.0g, 9.8 mmol), methyl iodide (2) (4.1g, 28 mmol), and acetone (2.4 ml) was heated at 60 °C with constant stirring for 8h. After cooling, the precipitate was filtered out, washed with dry ethyl ether (20 ml), and dried in the oven. Yellow powder; yield: 84 %. 1H NMR and 13C NMR spectra were consistent with the literature data. This can be represented as in Scheme 1.

ii. IL-tagged Schiff base (5)

The compound (5) was prepared from the method reported in the literature [45]. When compound (3) (249 mg, 10 mmol) was slowly added to an acidified clear solution of 2,4-dinitrophenylhydrazine (4) (198 mg, 1.0 mmol) in methanol. Within 5 min a yellowish precipitate was seen which was filtered out, washed with methanol, and dried in a hot air oven. Yield- 90 %, Elemental analysis calc. C 35.82 (36.30), H 2.06 (2.79), N 15.82 (16.43); Uv–Vis (in DMSO, nm) υ = 268 (π - π*), 391(η –π*); IR (KBr, cm^{-1}) υ = 3450 (m, br, –NH), 1619 (s, C═N), 1515 (*asym*, –NO_2), 1334 (*sym*, –NO_2), 1089 (-N-N-); ^{1}H NMR (400 MHz, DMSO-d_6, ppm): δ 12.024 (s, 1H,NH), δ 9.428 (s,1H,CH), 8.965 (d, 1H), 8.854 (t, 1H), 8.414 (q, 1H), δ 8.800 (s, 1H), δ 8.245 (d, 1H), δ 8.165 (d, 1H),δ 8.312 ppm (s, 1H, NCH), δ 4.413 (s, 3H,CH_3); ^{13}C NMR (400 MHz, DMSO-d_6, ppm): 146.014 (C^3), 144.524 ($C^{5/8}$), 142.371 ($C^{1/7}$), 138.948 (C^{11}), 134.592 (C^2), 131.435 (C^{10}), 130.167 (C^{13}), 128.360 (C^4), 123.400 (C^{12}), 117.906 (C^9), 48.834 (C^6); HRMS: molecular ion peak at m \z = 303.1030 (Calc. 303.0901). Degree of crystallinity = 78.62 %. Scheme 2 represents the synthesis of IL-tagged Schiff base ligand system.

iii. Metal complexes of IL-tagged Schiff base (6)

A reflux reaction in a 1:2 M ratio with respect to the metal salt and the ligand (5) was set up by slowly adding a clear solution of metal salts to a clear solution of ligand (5) in methanol at around 65 °C with constant stirring. The reaction continued for 30 min. The precipitate formed was filtered out, washed with cold methanol, and dried in a hot air oven at around 80 °C. Yellow powder; yield: 50–55 %. This can be seen in Scheme 3.

For Cu (II)-complex 6(a) [diacetoxybis(1-(2,4-dinitrophenyl-2-(1-methyl pyridine-1-ium-3-yl)methylene)hydrazineyl)copper iodide]; Elemental analysis calc. C 34.12 (34.65) H 2.83 (2.91) N 13.21 (13.47); UV–Vis (in DMSO, nm) υ = 265, 394 ($^2B_{1g} - {}^2E_g$, $^2B_{1g} - {}^2B_{2g}$); (IR (KBr, cm-1) υ = 3470 (-NH), 1633 (-C═N), 1508 (*asym*, -NO2), 1326 (*sym*, -NO2), 1096 (-N-N-), 544 (M − O), 426 (M − N), 1438-1159 (COO^{-1}). MALDI; molecular ion peak [M − 2I]+at m\z = 816.17 (calculated 816.25). Degree of crystallinity = 42.64 %.

For Zn (II)-complex 6(b) [diacetoxybis(1-(2,4-dinitrophenyl-2-(1-methyl pyridine-1-ium-3-yl)methylene)hydrazineyl)zinc iodide]; Elemental analysis calc. C 34.47 (34.59) H 2.83 (2.90) N 13.12 (13.44); UV–Vis (in DMSO, nm) υ = 266, 397 (MLCT or LMCT); IR (KBr, cm-1) υ = 3379 (-NH), 1627 (-C═N), 1510 (*asym*, -NO2), 1324 (*sym*, -NO2), 1098(-N-N-), 705 (M − O), 465(M − N), 1431-1162 (COO^{-1}). MALDI; molecular ion peak [M − 2I]+at m\z = 818.92 (calculated 819.08). Degree of crystallinity = 57.66 %.

For Cd (II)-complex 6(c) [diacetoxybis(1-(2,4-dinitrophenyl-2-(1-methyl pyridine-1-ium-3-yl)methylene)hydrazineyl)cadmium iodide]; Elemental analysis calc. C 32.75 (33.04) H 2.34 (2.78) N 12.34 (12.86); UV–Vis (in DMSO, nm) υ = 261, 395 (MLCT or LMCT); IR (KBr, cm-1) υ = 3290 (-NH), 1641 (C═N), 1509 (*asym*, -NO2), 1330 (*sym*, -NO2), 1103 (N–N), 683 (M − O), 429(M − N), 1398-1158(COO^{-1}). MALDI; molecular ion peak [M − 2I]+at m\z = 866.76 (calculated 866.12). Degree of crystallinity = 69.23 %

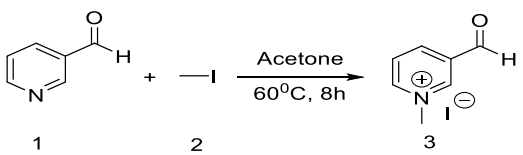

Scheme 1. Synthesis of pyridinium IL (3).

c.Biological studies

i.Cytotoxicity activity

In vitro cytotoxicity studies were carried out against the ACHN human renal adenocarcinoma cells which were procured from NCCS, PUNE (INDIA). The ACHN cell lines were cultured in 96 well microtiter plates in a humidified atmosphere of 5 % CO2 at 37 °C.

Cells were seeded at a density of 5×10^3 cells/well in 100 μl DMEM (Dulbecco's Modified Eagle Medium) culture medium for 24h. After 24h of incubation, the ligand (5) and its Cu (II)/Zn (II)/Cd (II)-complexes [6(a)/6(b)/6(c)] were added to each well at different concentrations ranging from 100 μl/ml to 400 μl/ml [e.g., 100 μl/ml, 150 μl/ml, 200 μl/ml, 250 μl/ml, 300 μl/ml, 350 μl/ml & 400 μl/ml in triplicate and incubated for another 24h. After the proper incubation period, the medium in the assay was replaced by a fresh medium containing 10 μl (5 mg/ml) of MTT powder dissolved in 1xPBS and further incubated for 3h at 37 °C. After incubation, 50 μl of isopropanol, formazan solubilizer was added to each well containing MTT and was shaken for about 10 min. The absorbance was then, recorded at 620 nm with DMSO as a blank in an ELISA reader. Indeed, DMSO concentrations were limited to 0.5 % (v/v) for this study which showed no significant effect on cell viability. Cytotoxicity activity was presented as a % of reduced MTT in treated cells vs-controlled cells incubated without drugs. The relative MTT level (%) was calculated by using the expression; Cytotoxicity % $= \left(\frac{X-Y}{X}\right) \times 100$ Where X is the mean optical density of control (untreated cells), Y is the mean optical density of treated cells with different drugs concentrations [46].

ii. ROS Assay

H_2DCFDA was used for the detection of hydrogen peroxide in the ACHN cell line. A standard protocol was performed with minor alterations for the assessment of intracellular ROS. The oxidation of 2, 7-dichlorofluorescein (H_2DCFDA) to 2, 7-dichlorodihydrofluorescein (H_2DCFDA) was monitored for the determination of hydrogen peroxide (H_2O_2). The human kidney cancer cell line (ACHN) was cultured on a coverslip in 35 mm Petri dishes. Plates were incubated for 24 h with 5 % CO_2 in an N-biotech incubator. After 24 h incubation, ACHN cells were treated with the previously determined IC_{50} concentration of each compound (from MTT assay). Control plates were kept without any treatment. The Cells were further incubated for 24 h under the same condition as mentioned above. The next day, plates were withdrawn and washed twice with phosphate buffer saline (PBS). H_2O_2 treatment was given to the positive control plate for 20 min 25 mM of fluorescence dye 2,7-dichlorofluorescein diacetate was given to all the plates and further incubated for 30 min. After that, cells were washed with 1X PBS to remove unbound dye. And glass slides were prepared by inverting cover slips on the slide in 20 % glycerin solution. Fluorescence was captured under an LED-based fluorescence microscope (Magnus MLXi) by using LED cassettes, samples were excited at 480 nm and using a long pass filter emission [47].

3. Results and discussions

A rigorous literature studies revels that there is hardly any single crystal data reported on the transition metal complexes having IL-tagged Schiff base as their ligand system. We also could not obtain any single crystal for our metal complexes. So, we had relied on tools other than single crystal XRD to assign appropriate geometry to the synthesized metal complexes.

3.1. Electronic spectra and magnetic moment measurements

Electronic Spectra of the ligand (5) and its Cu (II)/Zn (II)/Cd (II)-complexes [6(a)/6(b)/6(c)] were measured for the concentration of 1x 10^{-3}M in DMSO at room temperature in the range of 200–700 nm. The electronic spectrum of the ligand (5) shows absorption bands at 268 nm and 391 nm which were assigned to π - π * and n-π* transitions respectively. In the metal complexes these bands were shifted to different wavelength values thus suggesting a coordination between the metal ion and the ligand system as shown in Table 1 below.

In the electronic spectra of the Cu (II)-complex 6(a) these bands were shifted to 258 nm and 392 nm, in Zn (II)-complex 6(b) these bands were found at 265 nm and 395 nm and in Cd (II)-complex 6(c) the bands were at 262 nm and 398 nm. The bands at 540 nm in Cu (II)-complex 6(a) may be assigned to overlapping $^2B_{1g} \rightarrow {}^2A_{1g}$ and $^2B_{1g} - {}^2E_g$ transition transitions which is the characteristic band for a distorted square planar Cu (II)-complex. Hence, Cu (II)-complex 6(a) has been assigned a distorted square planar geometry. Further, its

Table 1
UV–Visible spectral data of the ligand (5) and its metal complexes (6).

Compound	Wavelength (nm)	Type of Transition
Ligand (5)	269	π-π*
	389	η-π*
Cu (II)-complex 6(a)	258	π-π*
	392	η-π*
	540	Overlapped $^2B_{1g} \rightarrow {}^2A_{1g}$ and $^2B1g \rightarrow {}^2Eg$
Zn (II)-complex 6(b)	265	π-π*
	395	η-π*
Cd (II)-complex 6(c)	262	π-π*
	398	η-π*

observed magnetic moment value of 1.83 B M. suggest the Cu (II)-complex 6(a) is mononuclear in nature.

Zn (II) and Cd (II) –complexes do not show d-d transition as their metal ions contain filled d-orbitals but they show charge transfer transition from metal ion to ligand or vice-versa. The observed bands in these complexes thus may be assigned to charge transfer transition between the metal ion and the ligand or vice-versa. Both these complexes were found to be diamagnetic in nature. So, they are assigned a tetrahedral geometry with coordination number of 4. UV–Visible specta of the ligand (5) and its metal complexes are shown below in Fig. 1.

3.2. Vibrational spectra

The FTIR spectrum of the free ligand (5) shows its distinctive bands at $\upsilon = 3450\ cm^{-1}$ and $\upsilon = 1619\ cm^{-1}$ which are assigned to N–H and C═N stretching vibrations respectively [Fig. 1, ESI†]. However, in the FTIR spectrum of the Cu (II)/Zn (II)/Cd (II)-complexes [6(a)/6(b)/6(c)] the υ (N–H) and υ (C═N) bands occur at 3470 cm^{-1}, 3379 cm^{-1}, 3290 cm^{-1} and 1633 cm^{-1}, 1627 cm^{-1}, 1641 cm^{-1} respectively [Fig. 1, ESI†]. Thus, there is a shift in the vibrational frequencies of the υ (N–H) and υ (C═N) bonds in Cu (II)/Zn (II)/Cd (II)-complexes [6(a)/6(b)/6(c)]. This confirms coordination between the metal ion and the ligand system through the nitrogen atom. Further, this is supported by the fact that there is a shift in υ (N–N) in Cu (II)/Zn (II)/Cd (II)-complexes [6(a)/6(b)/6(c)] slightly to a higher frequency (1096 cm^{-1},1098 cm^{-1} and 1103 cm^{-1}) as compared to that in the free ligand (5) (1089 cm^{-1}). Also, the anti-symmetric and symmetric vibrational frequencies of the carboxylate group (COO^{-}) in the metal complexes (6) lie in the range of 1438–1158 cm^{-1}. Such that the $\Delta\ \upsilon = [\upsilon_{asym}(\bar{COO}) - \upsilon_{sym}(\bar{COO})] = 280\ cm^{-1}$ substantiates the presence of the mono-dentate carboxylate group (COO^{-}) in the metal complexes (6) [48]. The appearance of bands in the range of 544–705 cm^{-1} and 426-465 cm^{-1} in the metal complexes (6) indicates the M − O and M − N stretching frequencies respectively. This suggests bonding of metal ion with the oxygen and nitrogen atom in the metal complexes. All the stretching frequencies of the ligand (5) and its metal complexes (6) are summarized in Table 2. And the FTIR spectrum of the ligand (5) and its metal complexes (6) can be seen in Fig. 1., ESI†.

3.3. NMR spectra

NMR spectra were recorded on Bruker 400 spectrometer operating at 400 MHz in DMSO-d_6. All the ^{1}H and ^{13}C NMR spectral data and the assignment of peaks in ligand (5) are stated in the experimental section 2.b.i and Fig. 2, Fig. 3, ESI†.

In the ^{1}H NMR spectrum of the ligand (5), a sharp peak at δ 12.024 ppm (s) is assigned to hydrazide (NH). And the peaks at δ 9.428 ppm (s), 8.965 ppm (d), 8.854 ppm (t), 8.414 ppm (d) are assigned to the pyridinium protons while the peaks at δ 8.800 ppm (s), 8.245 ppm (d), 8.165 (d) are assigned to benzene protons. The peak at δ 8.312 ppm (s) is assigned to aldimine proton (N═C–H) and the peak at δ 4.413 ppm (s) to methyl group (N–CH3).

3.4. HRMS

HRMS of the ligand (5) were recorded on Bruker micrOTOF-Q II spectrometer.

The molecular ion peak m\z at 303.1030 (calc. 303.0901) corresponds to $[M - I]^{+}$ion which supports the formation of the ligand (5). HRMS spectrum can be seen in Fig. 4 ESI†.

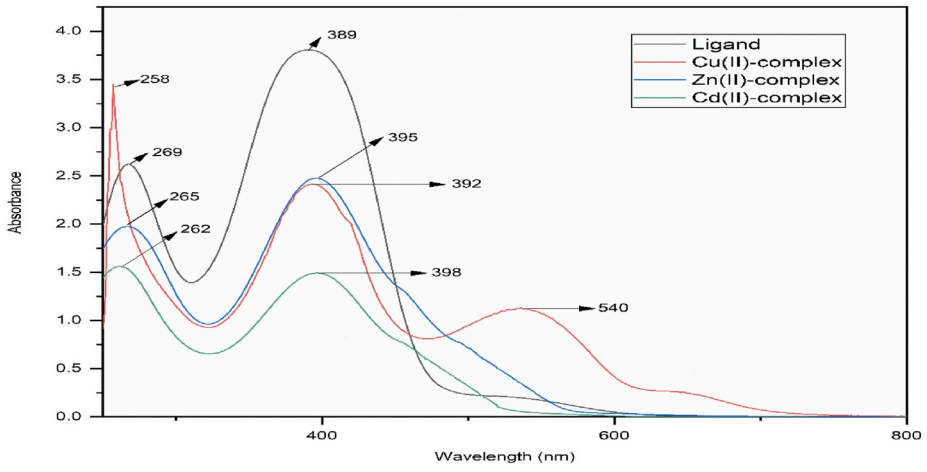

Fig. 1. (a)UV–Visible spectra of Ligand (5); Cu (II)-complex 6(a); Zn (II)-complex 6(b), and Cd (II)-complex 6(c) in DMSO (concentration of the solution = 1×10^{-3} M) at room temperature.

Table 2
Summary of important FTIR data of the ligand (5) and its metal complexes (6).

Sample	-C═N	-NH	-NN-	-NO_2	M-O	M-N	COO^-
Ligand (5)	1619	3450	1089	1515 (*asym*) 1334 (*sym*)	–	–	–
Cu (II)-complex 6(a)	1633	3470	1096	1508 (*asym*) 1326 (*sym*)	544	426	1438–1159
Zn (II)-complex 6(b)	1627	3379	1098	1510 (*asym*) 1324 (*sym*)	705	465	1431–1162
Cd-complex 6(c)	1641	3290	1103	1509 (*asym*) 1330 (*sym*)	683	429	1398–1158

[a]sym = symmetric; *asym* = asymmetric.

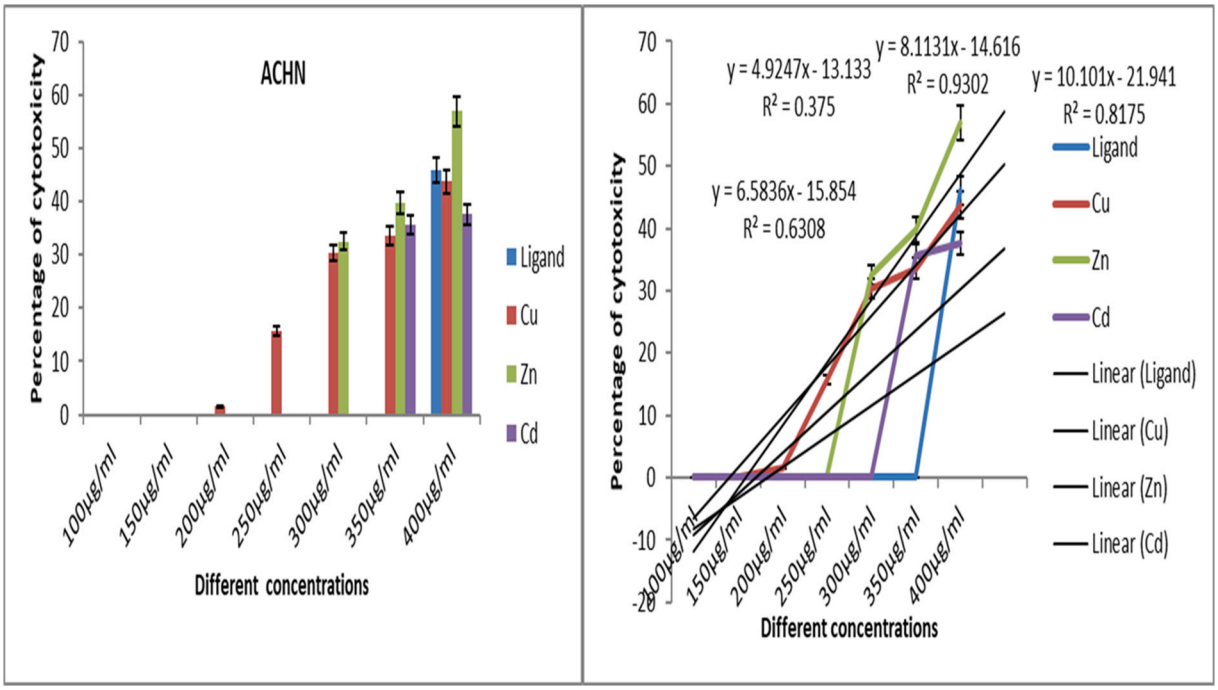

Fig. 2. (a) Concentration dependent cytotoxicity activity of the Ligand (5); Cu (II)-complex (6a); Zn (II)-complex (6b) and Cd (II)-complex (6c) against ACHN cell-line. (b) A plot of linear regression analysis of Ligand (5); Cu (II)-complex (6a); Zn (II)-complex (6b) and Cd (II)-complex (6c) to calculate their respective IC_{50} values against the ACHN cell-line.

3.5. MALDI

MALDI of Cu (II)/Zn (II)/Cd (II)-complexes [6(a)/6(b)/6(c)] were performed in Bruker Daltonics autoflex TOF/TOF instrument type. The MALDI spectrum of the Cu/Zn/Cd-complexes [6(a)/6(b)/6(c)] are shown in Figs. 5, Fig. 6, and Fig. 7 in ESI†. The [M − 2I]+ ion peaks are in good agreement with the proposed chemical formula of the Cu (II)/Zn (II)/Cd (II)-complexes [6(a)/6(b)/6(c)] with the peak values at *m/z* 816.17 (calculated 816.25), 818.92 (calculated 819.08), and 866.76 (calculated 866.12) respectively.

3.6. PXRD

PXRD was performed in PANalytical X-ray Diffractometer using Cu-κα radiation (1.54 A0) for the ligand (5) and its Cu (II)/Zn (II)/Cd (II)-complexes [6(a)/6(b)/6(c)] and the diffraction pattern were recorded over a range of 2θ angles from 10 to 80. Crystallite size and degree of crystallinity of the synthesized compounds were then determined from their respective PXRD data.

The PXRD pattern of the ligand (5) and its Cu (II)/Zn (II)/Cd (II)-complexes [6(a)/6(b)/6(c)] are shown in Figs. 8, Fig. 9, Fig. 10, Fig. 11 in ESI†. which exhibits sharp peaks at different 2θ values [2θ = 27.9890, 25.8907, 23.6708 for the ligand molecule (5); 27.6588, 25.2731, 19.5429, 14.7491 for Cu (II) –complex 6(a); 33.6789, 31.5830, 27.9710, 24.9609, 21.9509, 19.8550, 17.7591 for Zn (II)-complex 6(b) and 27.9710, 26.7670, 24.6711, 21.9509, 19.8550 for Cd (II)-complex 6(c)] indicating their crystalline nature. Also, a comparative study of the PXRD patterns of the ligand (5) and its Cu (II)/Zn (II)/Cd (II)-complexes [6(a)/6(b)/6(c)] shows the absence of or shifts in peaks at different 2θ in metal complexes from the ligand (5).

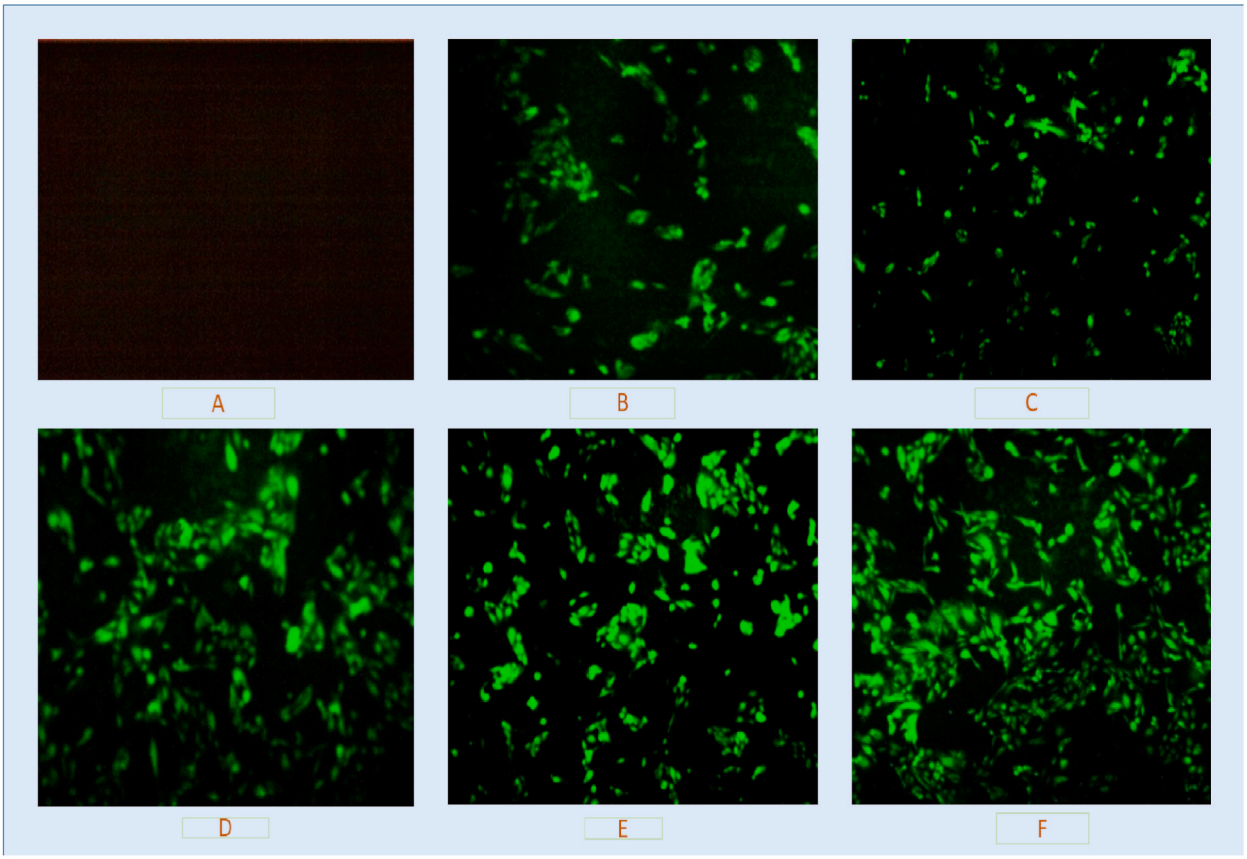

Fig. 3. Photomicrographs captured by using fluorescent probe DCF-DA at the end of the ROS assay of the four synthesized compounds against ACHN cell-line. A-Negative control (blank/untreated cell) where there was no ROS production. B-Positive control (H_2O_2) showing ROS production. C-Ligand (5) showing some ROS production. D- Cd (II)-complex (6c) showing more ROS production compare to ligand (5). E-Cu (II)-complex (6a) showing more ROS production compare to Cd (II)-complex (6c). F–Zn (II)-complex showing the highest ROS production.

The crystallite size of the ligand (5) and its Cu (II)/Zn (II)/Cd (II)-complexes [6(a)/6(b)/6(c)] were found to be 0.42 nm, 0.36 nm, 0.34 nm, and 0.29 nm respectively as calculated by Scherrer's Equation;

$$\text{Crystallite size}, D(nm) = \kappa\lambda/\beta\, cos\, \theta$$

Where $\kappa = 0.9$ (Scherrer's Constant), $\lambda = 0.154$ nm (wavelength of the X-ray source), β = FWHM (radians), θ = Peak position (radians) and their degree of crystallinity was found to be 78.62 %, 42.64 %, 57.66 %, and 69.23 % respectively as given by,

$$\text{Degree of Crystallinity } (\%) = \frac{\text{Area of crystalline peaks}}{\text{area of all peaks}} \times 100$$

This result shows the loss in the crystalline nature of the ligand (5) on metalation with the metal ions.

4. Biological studies

4.1. Cytotoxicity activity

MTT assay is done to measure the toxicity of a drug that interferes with the cellular viability. The well-known cytotoxic drugs targets and interfere with the reproducibility of cells to control their growth and proliferation. In short, the toxicity of drugs or any treatment is inversely proportional to the cell viability. Here, the toxicity of the samples is proved to be concentration dependent as it decreases the viability of cells along with increasing drug concentrations. No observable toxicity was seen at concentrations below 200 μl/ml of the sample as these compounds may be opted out from the treated cells by the cells own defense mechanism. The percentage of cell viability of treated cells indicate that some of the drugs can interfere with their reproducibility in a distinct way. The ligand showed no toxicity against the cancer cell line concentrations ranging from 100 to 350 μg/ml. At higher concentration, the ligand (5) shows some toxicity that eventually leads to the decrease in cellular viability. On the other hand, Cu (II)/Zn (II)/Cd (II)-complexes (6a/6b/6c) showed toxicity greater than the ligand (5). The significant drug toxicity of Cu (II)-complex (6a) was observed at 200 μg/ml

concentration and found to increase with increasing concentration. Other two drugs (Zn (II)/Cd (II)-complexes) (6b/6c) also hinder cellular viability. Among all the drugs being tested, cytotoxicity caused by Zn (II)-complex (6b) is much higher when compared with others. Zn (II) ions activates some cellular stress on cells and altered its response in case of high dose exposure that ultimately led to cell death or it directly inhibits the cellular ability to replicate under this treatment. But, by which mechanism this drug confer cellular death is not apparent. Hence some detailed study in this direction is needed. The differences in the cell reducing capabilities of drugs are mainly dependent on their targets in a cell and thus cellular responses are non-identical and vary from one cell to another. The graph shows (Fig. 2) that the Zn (II)-complex (6b) is capable of inducing cytotoxicity on cancer cells. The IC_{50} value calculated from the graph (Fig. 2) indicates different doses that is necessary for reducing cellular viability to its 50 % concentration. The IC_{50} data is represented on a separate table (Table 3). This concentration also proved the fact that among all the drugs under test, Zn (II)-complex (6b) can induce more toxicity to cancer cells due to its low IC_{50} (7.12 μg/ml) value when compared with others. Cu (II) –complex (6a) and Cd (II) –complex (6c) also confers cytotoxicity with IC_{50} value of 7.97 μg/ml and 10 μg/ml respectively. The IC_{50} value (12.82 μg/ml) of ligand (5) comprises the finding that it can induce toxicity to cancer cell but at a higher concentration. Elaborated investigation should be conducted in this track to fulfil the need of achieving potent cytotoxic properties of the drug which can specifically reduce the cancer cell reproducibility.

ii. ROS (Reactive Oxygen Species) production

There was no significant internal ROS production in control (blank) as shown in Fig. 3 A and ROS production was enhanced in the presence of H_2O_2 which is taken as a positive control for this ROS assay as seen in Fig. 3 B. The cells treated with IC_{50} value of Zn (II)-complex (6b) showed observable ROS production compare to that of the ligand (5) as seen in Fig. 3 F and Fig. 3C. The intensity of fluorescence thus increased in presence of Zn (II) ion. Thus, Zn (II)-complex (6b) shows the synergic effect in ROS production. Such effect was also seen in other two metal complexes Cu (II)-complex (6a) in Fig. 3. E and Cd (II)-complex (6c) in Fig. 3 D. But, the IC_{50} values of Cu (II)-complex (6a) and Cd (II)-complex (6c) are slightly higher for inducing ROS in cancer cell compared to Zn (II)-complex (6b). The higher ROS production indicates the fact that Zn (II)-complex (6b) induces some sort of cellular stress in greater magnitude compare to Cu (II)-complex (6a) and Cd (II)-complex (6c) that ultimately leads to higher reactive oxygen species (ROS) formation. Thus, the excessive ROS formation in cancer cells causes to loss its cellular reproducibility under the treatment [39].

5. Conclusion

We handout a novel Pyridinium iodide-tagged Schiff base (5) and its Cu (II)/Zn (II)/Cd (II)-complexes (6) to the scientific community as an active compound against the ACHN human renal adenocarcinoma cell line. The synthesized compounds have been well characterized by Elemental analysis, UV–Visible Spectroscopy, FTIR Spectroscopy, NMR spectroscopy, Mass Spectroscopy, Magnetic Susceptibility and PXRD. Among these compounds the cytotoxicity activity activities decrease in the order Zn (II)-complex 6(b) [IC_{50} value7.12 μg/ml] > Cu (II)-complex 6(a) [IC_{50} value7.97 μg/ml] > Cd (II)-complex 6(c) [IC_{50} value 10.00 μg/ml]> Ligand (5) [IC_{50} value 12.82 μg/ml]. And this activity order is in good agreement with the results of their ROS assay. From this observation we conclude that there is a synergistic effect of the ligand (5) and the Cu (II)/Zn (II)/Cd (II)-ions towards their cytotoxicity activity against the ACHN cell line. In other words, the synthesis of the pyridinium IL-tagged Schiff base and its metal complexes have been a fruitful purpose.

Data availability statement

The data that support the finding of this study are available on request from the corresponding author.

CRediT authorship contribution statement

Pranesh Rai: Writing – review & editing, Writing – original draft, Visualization, Validation, Software, Methodology, Investigation, Funding acquisition, Formal analysis, Data curation, Conceptualization. **Ankita Dutta:** Validation, Software, Methodology, Investigation, Formal analysis, Data curation, Conceptualization. **Anoop Kumar:** Visualization, Validation, Supervision, Project administration, Methodology, Investigation, Formal analysis, Data curation, Conceptualization. **Biswajit Sinha:** Writing – review & editing, Visualization, Validation, Supervision, Software, Resources, Project administration, Methodology, Investigation, Funding acquisition, Formal analysis, Data curation, Conceptualization.

Declaration of generative AI and AI-assisted technologies in the writing process

During the preparation of this article, we used Quillbot and Grammarly softwares (Free versions) to improve writing skills and to check grammatical errors. After using these softwares, we reviewed and edited the content as needed and take(s) full responsibility for the content of the publication.

Declaration of competing interest

The authors declare that they have no known competing financial interests or personal relationships that could have appeared to

Table 3
Calculated IC_{50} values of Ligand (5); Cu (II)-complex (6a); Zn (II)-complex (6b) and Cd (II)-complex (6c) against ACHN cell-line.

Sample	Ligand (5)	Cu (II)-complex (6a)	Zn (II)-complex (6b)	Cd (II)-complex (6c)
IC_{50}	12.82 μg/ml	7.97 μg/ml	7.12 μg/ml	10 10.00 μg/ml

influence the work reported in this paper.

Acknowledgement

The authors thank Mr. Pramod Rai, IISER-KOL, India for HRMS and his constant support; BSBE, IIT-B, India for MALDI Facility; Mr. Sagarmani Rasaily and Mr. Debesh Sharma for PXRD, Sikkim University, India; Dr. Mayukh Deb for NMR, Dept. Of Chemistry, University of North Bengal, India and the Departmental Special Assistance Scheme under the University Grants Commission, New Delhi [DRS-SAP_III, N0. F540/12/DRS/2013] for financial support.

Appendix A. Supplementary data

Supplementary data to this article can be found online at https://doi.org/10.1016/j.heliyon.2024.e25246.

References

[1] N.V. Plechkova, K.R. Seddon, Applications of ionic liquids in the chemical industry, Chem. Soc. Rev. 37 (2008) 123–150, https://doi.org/10.1039/b006677j.
[2] Z. Lei, B. Chen, Y.M. Koo, D.R. Macfarlane, Introduction: ionic liquids, Chem. Rev. 117 (2017) 6633–6635, https://doi.org/10.1021/acs.chemrev.7b00246.
[3] R.D. Rogers, K.R. Seddon, Ionic liquids - solvents of the future? Science 80 (2003) 792–793, https://doi.org/10.1126/science.1090313, 302.
[4] R.A. Sheldon, Green solvents for sustainable organic synthesis: state of the art, Green Chem. 7 (2005) 267–278, https://doi.org/10.1039/b418069k.
[5] P. Wasserscheid, W. Keim, Ionic LiquidsDNew [a]solutions[o] for transition metal catalysis, Angew. Chem. Int. Ed. 39 (2000) 3772–3789.
[6] A.J. Carmichael, M.J. Earle, J.D. Holbrey, P.B. McCormac, K.R. Seddon, The Heck reaction in ionic liquids: a multiphasic catalyst system, Org. Lett. 1 (1999) 997–1000, https://doi.org/10.1021/ol9907771.
[7] B. Khungar, M.S. Rao, K. Pericherla, P. Nehra, N. Jain, J. Panwar, A. Kumar, Synthesis, characterization and microbiocidal studies of novel ionic liquid tagged Schiff bases, Compt. Rendus Chem. 15 (2012) 669–674, https://doi.org/10.1016/j.crci.2012.05.023.
[8] P. Nehra, B. Khungar, K. Pericherla, S.C. Sivasubramanian, A. Kumar, Imidazolium ionic liquid-tagged palladium complex: an efficient catalyst for the Heck and Suzuki reactions in aqueous media, Green Chem. 16 (2014) 4266–4271, https://doi.org/10.1039/c4gc00525b.
[9] S. Saha, D. Brahman, B. Sinha, Cu(II) complexes of an ionic liquid-based Schiff base [1-{2-((2-hydroxybenzylidene)amino)ethyl}-3-methylimidazolium] PF6: synthesis, characterization and biological activities, J. Serb. Chem. Soc. 80 (2015) 35–43, https://doi.org/10.2298/JSC140201078S.
[10] A. Chhetri, S. Chettri, P. Rai, D.K. Mishra, B. Sinha, D. Brahman, Synthesis, characterization and computational study on potential inhibitory action of novel azo imidazole derivatives against COVID-19 main protease (Mpro: 6LU7), J. Mol. Struct. 1225 (2021) 129230, https://doi.org/10.1016/j.molstruc.2020.129230.
[11] A. Chhetri, S. Chettri, P. Rai, B. Sinha, D. Brahman, Exploration of inhibitory action of Azo imidazole derivatives against COVID-19 main protease (Mpro): a computational study, J. Mol. Struct. 1224 (2021), https://doi.org/10.1016/j.molstruc.2020.129178.
[12] S. Sowmiah, J.M.S.S. Esperança, L.P.N. Rebelo, C.A.M. Afonso, Pyridinium salts: from synthesis to reactivity and applications, Org, Chem. Front. 5 (2018) 453–493, https://doi.org/10.1039/c7qo00836h.
[13] V. Alptüzün, S. Parlar, H. Taşli, E. Erciyas, Synthesis and antimicrobial activity of some pyridinium salts, Molecules 14 (2009) 5203–5215, https://doi.org/10.3390/molecules14125203.
[14] S. Omidi, V. Khojasteh, A. Kakanejadifard, M. Ghasemian, F. Azarbani, Synthesis, characterization, spectroscopy and biological activity of 4-((3-formyl-4-hydroxyphenyl)azo)-1-alkylpyridinium salts, J. Chem. Sci. 130 (2018), https://doi.org/10.1007/s12039-018-1521-5.
[15] T. Sciences, Akademia baru journal of advanced research in fluid synthesis and characterization of new cholinium-based ionic liquids for antimicrobial application, Akademia Baru 1 (2018) 16–23.
[16] D. Hodyna, V. Kovalishyn, I. Semenyuta, S. Rogalsky, O. Trokhimenko, A. Gryniukova, L. Metelytsia, Ester-functionalized imidazolium-and pyridinium-based ionic liquids: design, synthesis and cytotoxicity evaluation, Biointerface Res. Appl. Chem. 12 (2022) 2905–2957, https://doi.org/10.33263/BRIAC123.29052957.
[17] M. Musiał, A.B. Olejniczak, M. Denel-Bobrowska, E. Zorębski, M. Dzida, In vitro anticancer and antivirus activities of cyano- and bis(trifluoromethylsulfonyl) imide-based ionic liquids, ACS Sustain. Chem. Eng. 9 (2021) 16459–16465, https://doi.org/10.1021/acssuschemeng.1c06580.
[18] K.S. Egorova, E.G. Gordeev, V.P. Ananikov, Biological activity of ionic liquids and their application in pharmaceutics and medicine, Chem. Rev. 117 (2017) 7132–7189, https://doi.org/10.1021/acs.chemrev.6b00562.
[19] V.R.R.K. Dasari, M.K.K. Muthyala, M.Y. Nikku, S.R.R. Donthireddy, Novel Pyridinium compound from marine actinomycete, Amycolatopsis alba var. nov. DVR D4 showing antimicrobial and cytotoxic activities in vitro, Microbiol. Res. 167 (2012) 346–351, https://doi.org/10.1016/j.micres.2011.12.003.
[20] T. Turk, R. Frangež, K. Sepčić, Mechanisms of toxicity of 3-alkylpyridinium polymers from marine sponge reniera sarai, Mar. Drugs 5 (2007) 157–167. www.mdpi.org/marinedrugs.
[21] Mol Donahoe, Cell. Biochem. 23 (2012) 1–7, https://doi.org/10.3892/ijo.2010.863.
[22] A. Pradhan, A. Kumar, A review: an overview on synthesis of some Schiff bases and there metal complexes with anti-microbial activity, Chem. Process Eng. Res. 35 (2015) 84–87.
[23] M. Saddam Hossain, M. Nuruzzaman Khan, C. Md Zakaria, S. Afrin Dalia, B. Farhana Afsan, B. Md Saddam Hossain, B. Md Kudrat-E-Zahan, B. Md Mohsin Ali, C. Md Kudrat-E-Zahan, F. Afsan, C. Zakaria, M. Kudrat-E-Zahan, M. Mohsin Ali, A short review on chemistry of schiff base metal complexes and their catalytic application Evaluation of groundwater quality View project schiff base View project A short review on chemistry of schiff base metal complexes and their catalytic application, Int. J. Chem. Stud. 6 (2018). https://www.researchgate.net/publication/325845095.
[24] K. Andiappan, A. Sanmugam, E. Deivanayagam, K. Karuppasamy, H.S. Kim, D. Vikraman, In vitro cytotoxicity activity of novel Schiff base ligand-lanthanide complexes, Sci. Rep. 8 (2018), https://doi.org/10.1038/s41598-018-21366-1.
[25] R. Induleka, A. C P, M. Tamilselvi, S. Ushanandhini, M. Gowri, Evaluation of Anticancer Activity of Schiff Bases Derived from Pyridine and Their Metal Complexes (A Review), 2022.
[26] N. Fahmi, S. Shrivastava, R. Meena, S.C. Joshi, R.V. Singh, Microwave assisted synthesis, spectroscopic characterization and biological aspects of some new chromium(iii) complexes derived from NO donor Schiff bases, New J. Chem. 37 (2013) 1445–1453, https://doi.org/10.1039/c3nj40907d.

[27] S. Omidi, A. Kakanejadifard, A review on biological activities of Schiff base, hydrazone, and oxime derivatives of curcumin, RSC Adv. 10 (2020) 30186–30202, https://doi.org/10.1039/d0ra05720g.
[28] A.T. Chaviara, P.C. Christidis, A. Papageorgiou, E. Chrysogelou, D.J. Hadjipavlou-Litina, C.A. Bolos, In vivo anticancer, anti-inflammatory, and toxicity studies of mixed-ligand Cu(II) complexes of dien and its Schiff dibases with heterocyclic aldehydes and 2-amino-2-thiazoline. Crystal structure of [Cu(dien)(Br)(2a-2tzn)](Br)(H 2O), J. Inorg. Biochem. 99 (2005) 2102–2109, https://doi.org/10.1016/j.jinorgbio.2005.07.011.
[29] S.N. Pandeya, P. Yogeeswari, D. Sriram, E. De Clercq, C. Pannecouque, M. Witvrouw, Synthesis and screening for anti-HIV activity of some N-Mannich bases of isatin derivatives, Chemotherapy 45 (1999) 192–196, https://doi.org/10.1159/000007182.
[30] C.M. Da Silva, D.L. Da Silva, L.V. Modolo, R.B. Alves, M.A. De Resende, C.V.B. Martins, Â. De Fátima, Schiff bases: a short review of their antimicrobial activities, J. Adv. Res. 2 (2011) 1–8, https://doi.org/10.1016/j.jare.2010.05.004.
[31] M.S. Mashhoori, R. Sandaroos, A. Zeraatkar Moghaddam, Design of a new poly imidazolium-tagged cobalt (II) schiff base complex for selective oxidation of alcohols and sulfides in a water solvent, Polycycl. Aromat. Comp. 0 (2021) 1–19, https://doi.org/10.1080/10406638.2021.1922470.
[32] C. Bibal, J.C. Daran, S. Deroover, R. Poli, Ionic Schiff base dioxidomolybdenum(VI) complexes as catalysts in ionic liquid media for cyclooctene epoxidation, Polyhedron 29 (2010) 639–647, https://doi.org/10.1016/j.poly.2009.09.001.
[33] M.V. Khedkar, T. Sasaki, B.M. Bhanage, Immobilized palladium metal-containing ionic liquid-catalyzed alkoxycarbonylation, phenoxycarbonylation, and aminocarbonylation reactions, ACS Catal. 3 (2013) 287–293, https://doi.org/10.1021/cs300719r.
[34] R.F.M. Elshaarawy, C. Janiak, Ionic liquid-supported chiral saldach with tunable hydrogen bonding: synthesis, metalation with Fe(III) and in vitro antimicrobial susceptibility, Tetrahedron 70 (2014) 8023–8032, https://doi.org/10.1016/j.tet.2014.08.034.
[35] M.S. Mashhoori, R. Sandaroos, A. Zeraatkar Moghaddam, Polymeric imidazolium ionic liquid-tagged manganese Schiff base complex: an efficient catalyst for the Biginelli reaction, Res. Chem. Intermed. 46 (2020) 4939–4954, https://doi.org/10.1007/s11164-020-04230-8.
[36] S. Saha, G. Basak, B. Sinha, Physico-chemical characterization and biological studies of newly synthesized metal complexes of an Ionic liquid-supported Schiff base: 1-{2-[(2-hydroxy-5-bromobenzylidene)amino]ethyl}-3-ethylimidazolium tetrafluoroborate, J. Chem. Sci. 130 (2018), https://doi.org/10.1007/s12039-017-1409-9.
[37] F.E. Bennani, L. Doudach, K. Karrouchi, Y. El rhayam, C.E. Rudd, M. Ansar, M. El Abbes Faouzi, Design and prediction of novel pyrazole derivatives as potential anti-cancer compounds based on 2D-2D-QSAR study against PC-3, B16F10, K562, MDA-MB-231, A2780, ACHN and NUGC cancer cell lines, Heliyon 8 (2022), https://doi.org/10.1016/j.heliyon.2022.e10003.
[38] Jyoti Subhash, A. Phor, A. Chaudhary, Synthesis, Structural elucidation, cytotoxic, antimicrobial, antioxidant, density functional theory and molecular docking studies of mononuclear Ru(II) complexes of N4O4-bearing macrocyclic ligands, J. Inorg. Organomet. Polym. Mater. (2023), https://doi.org/10.1007/s10904-023-02862-y.
[39] Jyoti Subhash, A. Chaudhary, Synthesis, Spectroscopic characterization, in vitro cytotoxic, antimicrobial and antioxidant studies of Co(II) complexes bearing pyridine-based macrocyclic ligands with density function theory (DFT) and molecular docking investigations, Res. Chem. Intermed. 49 (2023) 4729–4758, https://doi.org/10.1007/s11164-023-05096-2.
[40] Jyoti Subhash, M. Gupta, A. A Phor, Synthesis Chaudhary, Spectral characterisation, in vitro cytotoxicity, antimicrobial, antioxidant, DFT and molecular docking studies of Ru(III) complexes derived from amide-based macrocyclic ligands, Res. Chem. Intermed. (2023), https://doi.org/10.1007/s11164-023-05124-1.
[41] A. Chaudhary Subhash, Jyoti Mamta, Synthesis, structural characterization, thermal analysis, DFT, biocidal evaluation and molecular docking studies of amide-based Co(II) complexes, Chem. Pap. 77 (2023) 5059–5078, https://doi.org/10.1007/s11696-023-02843-y.
[42] A. Chaudhary, M. Kumar, N. Kumar, N.K. Agarwal, Synthesis, Spectroscopic Characterization, Biocidal evaluation Molecular Docking & DFT Investigation of 16-18 membered Macrocyclic Complexes of Cobalt (II). https://doi.org/10.1007/s12039-022, 2020.
[43] A. Subhash, Jyoti Chaudhary, Mamta M Kumar, R. Solanki, Synthesis, structural elucidation, DFT investigations, biological evaluation and molecular docking studies of tetraamide-based macrocyclic cobalt (II) complexes, J. Iran. Chem. Soc. 20 (2023) 2339–2362, https://doi.org/10.1007/s13738-023-02847-1.
[44] S.A. Hosseini, A. Moghimi, M. Iman, F. Ebrahimi, Docking studies, synthesis, and in-vitro evaluation of novel oximes based on nitrones as reactivators of inhibited acetylcholinesterase, Iran, J. Pharm. Res. 16 (2017) 880–892.
[45] H.H. Monfared, O. Pouralimardan, C. Janiak, Synthesis and spectral characterization of hydrazone schiff bases derived from 2,4-dinitrophenylhydrazine. Crystal structure of salicylaldehyde-2,4- dinitrophenylhydrazone, Zeitschrift Fur Naturforsch. - Sect. B J. Chem. Sci. 62 (2007) 717–720, https://doi.org/10.1515/znb-2007-0515.
[46] E. Bursal, F. Turkan, K. Buldurun, N. Turan, A. Aras, N. Çolak, M. Murahari, M.C. Yergeri, Transition metal complexes of a multidentate Schiff base ligand containing pyridine: synthesis, characterization, enzyme inhibitions, antioxidant properties, and molecular docking studies, Biometals 34 (2021) 393–406, https://doi.org/10.1007/s10534-021-00287-z.
[47] P. Bomzan, N. Roy, A. Sharma, V. Rai, S. Ghosh, A. Kumar, M.N. Roy, Molecular encapsulation study of indole-3-methanol in cyclodextrins: effect on antimicrobial activity and cytotoxicity, J. Mol. Struct. 1225 (2021), https://doi.org/10.1016/j.molstruc.2020.129093.
[48] M. Khawar Rauf, M. Adeel Saeed, Imtiaz-ud-Din, M. Bolte, A. Badshah, B. Mirza, Synthesis, characterization and biological activities of some new organotin(IV) derivatives: crystal structure of [(Sn Ph3) (OOCC6H4OH)] and [(SnMe3)2 (OOC)2C6Cl4 (DMSO)2], J. Organomet. Chem. 693 (2008) 3043–3048, https://doi.org/10.1016/j.jorganchem.2008.06.027.